

# Measurement of the Entropy and Critical Temperature of a Strongly Interacting Fermi Gas

L. Luo, B. Clancy, J. Joseph, J. Kinast, and J. E. Thomas

<sup>1</sup>Physics Department, Duke University, Durham, North Carolina 27708-0305, USA

To whom correspondence should be addressed; E-mail: jet@phy.duke.edu.

(Submitted 21 November, 2006)

**We report a model-independent measurement of the entropy, energy, and critical temperature of a degenerate, strongly interacting Fermi gas of atoms. The total energy is determined from the mean square cloud size in the strongly interacting regime, where the gas exhibits universal behavior. The entropy is measured by sweeping a bias magnetic field to adiabatically tune the gas from the strongly interacting regime to a weakly interacting regime, where the entropy is known from the cloud size after the sweep. The dependence of the entropy on the total energy quantitatively tests predictions of the finite-temperature thermodynamics.**

Strongly interacting Fermi gases are of great interest, as they exhibit universal thermodynamic behavior, where the properties are independent of the details of the microscopic interactions (1, 2, 3, 4). These gases provide models for testing nonperturbative many-body theories in

a variety of fields from neutron stars and nuclear matter (5, 6, 2, 7) to quark-gluon plasmas (8) and high temperature superconductors (9). Hence, thermodynamic experiments on strongly interacting Fermi gases are of great importance.

In studies of the thermodynamics of these systems, where thermometry is difficult (10), entropy measurement plays a central and fundamental role. We report the measurement of the entropy  $S$  of a strongly interacting Fermi gas as a function of its total energy  $E$ . The results yield the temperature  $T$  via the elementary thermodynamic relation  $1/T = \partial S / \partial E$ . Our experiments quantitatively test recent predictions of the entropy based on microscopic many-body theory, yield the dependence of the energy on temperature, and determine the critical temperature for the superfluid transition without invoking any specific theoretical model.

Strongly-attractive Fermi gases exhibit both fermionic and bosonic features, and have been studied intensely for several years in theory (11, 12, 13, 9) and experiment (1, 14, 15, 16, 17, 18, 19). Measurements of the heat capacity (20) and collective mode damping versus energy (21) reveal transitions in behavior, which have been interpreted as a superfluid transition in this system (20). Recently, the observation of vortices (22) has provided a definitive proof of a superfluid phase. However, there have been no model-independent studies of the thermodynamic properties.

A strongly interacting Fermi gas is prepared using a 50:50 mixture of the two lowest hyperfine states of  $^6\text{Li}$  atoms in an ultrastable  $\text{CO}_2$  laser trap with a bias magnetic field of 840 G just above a broad Feshbach resonance at  $B = 834$  G (23). The gas is cooled to quantum degeneracy by lowering the trap depth by a factor of  $\sim 1000$  (1). Following forced evaporation, the trap depth  $U_0$  is recompressed to  $U_0/k_B = 10$  K, which is large compared to the energy per particle of the gas. Here  $k_B$  is the Boltzmann constant. After this procedure, the initial energy is close to that of the ground state, as described below.

At the final trap depth, the measured trap oscillation frequencies in the transverse directions are  $\nu_x = 2\pi \times 670$  Hz and  $\nu_y = 2\pi \times 760$  Hz, while the axial frequency is  $\nu_z = 2\pi \times 30$

Hz @ 840 G and  $\omega_z = 2\pi \times 32$  Hz @ 1200 G. Note that axial frequencies differ due to the small change in the trapping potential arising from the bias magnetic field curvature. The total number of atoms  $N = 1.3(0.2) \times 10^5$  is obtained from absorption images of the cloud using a two-level optical transition at 840 G. The corresponding Fermi energy  $E_F$  and Fermi temperature  $T_F$  for an ideal (noninteracting) harmonically trapped gas at the trap center are  $E_F = k_B T_F \sim \frac{1}{2} (3N)^{1/3}$ , where  $\omega = (\omega_x \omega_y \omega_z)^{1/3}$ . For our trap conditions, we obtain  $T_F = 1.0$  K.

The total energy per particle,  $E$ , of the strongly interacting gas is measured in a model-independent way from the mean square size in the axial direction (4). In this strongly interacting regime, the zero energy s-wave scattering length  $a_s$  is large compared to the interparticle spacing, which is large compared to the range of the two-body interaction, so that the gas is universal (2, 1, 3). Then, the local pressure is  $P = 2E/3$ , where  $E$  is the local energy density (3, 4). Using force balance for a trapping potential  $U$ ,  $r P + n r U = 0$ , where  $n$  is the local density, one then obtains the total energy per particle  $E = \frac{3}{2} m \omega_z^2 \bar{z}_{840}^2 (1 + \delta)$  or

$$\frac{E}{E_F} = \frac{\hbar \omega_z^2 \bar{z}_{840}^2}{z_F^2} (1 + \delta); \quad (1)$$

where  $\hbar \omega_z^2 \bar{z}_{840}^2$  is the mean square axial cloud size measured at 840 G and  $m$  is the  $^6\text{Li}$  mass. Here,  $z_F^2$  is defined by  $\frac{3}{2} m \omega_z^2 z_F^2 = E_F$ , and is weakly dependent on the magnetic field through the trap frequencies. The correction factor  $1 + \delta$  arises from anharmonicity (24) in the shallow trapping potential  $U_0 = 10 E_F$  used in the experiments. We find that  $\delta$  varies from 3% at our lowest energies to 13% at the highest.

The entropy of the strongly interacting gas at 840 G is determined using an adiabatic sweep of the magnetic field to a relatively weakly-interacting regime at 1200 G, where a reference entropy can be estimated from the mean square axial cloud size  $\hbar \omega_z^2 \bar{z}_{1200}^2$ . At 1200 G,  $a_s = 2900$  bohr (23), and  $k_F a_s = 0.75$  for our shallow trap, with  $k_F = \sqrt{\frac{P}{2m k_B T_F}}$ . At

$k_F a = 0.75$ , we expect that the dependence of the entropy on the cloud size should be close to that of an ideal noninteracting Fermi gas with primarily a small mean-field reduction in the ground state cloud size. This conjecture is supported by the observed ballistic expansion of the cloud at 1200 G, even at our lowest temperatures, which shows that the gas is nearly normal. We also find that the calculated ideal gas entropy differs from a many-body result for  $k_F a_S = 0.75$  (25) by less than 1% over the range of energies we studied, except at the point of the lowest energy, where they differ by 10%. For this comparison, we slightly shift the ground state size of the ideal gas to coincide with that calculated for  $k_F a_S = 0.75$ . Hence, the reference entropy at 1200 G is nearly identical in shape to that for an ideal gas, and provides a model-independent estimate of the entropy of the strongly interacting gas.

Ideally, a sweep from 840 G to a magnetic field of 528 G, where the scattering length vanishes, would produce a noninteracting gas ( $k_F a_S = 0$ ), where the entropy is precisely known. Unfortunately, adiabatic formation of molecules (26) and subsequent molecular decay at fields below resonance (17) cause unwanted heating for such a downward sweep.

To measure the entropy as a function of energy, we start with an energy near the ground state and controllably increase the energy of the gas by releasing the cloud for an adjustable time and then recapturing it, as described previously (20). After recapture, the gas is allowed to reach equilibrium for 0.7 s. This thermalization time is omitted for measurement of the ground state size, where no energy is added.

After equilibrium is established, the magnetic field is either ramped to 1200 G over a period of 1 s, or the gas is held at 840 G for 1 s. In either case, after 1 s, the gas is released from the trap for a short time to increase the transverse dimension of the cloud for imaging, without significantly changing (less than 0.5%) the measured axial cloud size.

We find that the magnetic field sweep is nearly adiabatic, since the mean square size of the cloud at 840 G after a round-trip-sweep of 2 s duration is found to be within 3% of that

obtained after a hold time of 2 s at 840 G. However, we also find for our shallow trap that there is a magnetic field and energy independent heating rate, which causes the mean square size to slowly increase at a rate of  $\hbar z_F^2 \dot{z} = 0.024 z_F^2 \text{ s}^{-1}$ , corresponding to 24 nK/s in energy units. Since we desire the energy and entropy just after equilibration, we subtract  $\hbar z_F^2 \dot{z} \times 1 \text{ s}$  from the measured mean square axial dimensions for both the 840 G and 1200 G data. The maximum correction is 5% at the lowest energies.

Fig. 1 shows the ratio of the mean square axial cloud size at 1200 G (measured after the sweep) to that at 840 G (measured prior to the sweep), as a function of the energy of the strongly interacting gas at 840 G. The energy at 840 G is directly measured from the axial cloud size at 840 G using Eq. 1. The displayed ratio and energy scale are independent of the atom number and trap parameters. This is accomplished by measuring the mean square sizes at each field in units of  $z_F^2$  for the given field and atom number. The total data comprise 900 measurements which have been averaged in energy bins of width  $\Delta E = 0.04 E_F$ .

The red solid line shows the predictions obtained by equating the entropies calculated at 1200 G and near resonance (25). The predicted curve exhibits a rapid drop followed by a slower decline to unity, in very good agreement with the data in the low and high energy regions. However, the data deviate significantly from the prediction in the region centered near  $E = E_0 + 0.4 E_F$ , where the entropy changes behavior as described below.

We note that potential energy has been measured previously in  $^{40}\text{K}$  (27) at a Feshbach resonance and after an adiabatic sweep to the noninteracting regime. In Ref. (27), the resulting potential energy ratios are given as a function of the temperature of the noninteracting gas. In contrast, by exploiting universality, our cloud size ratios are referred to the total energy in the strongly interacting regime, which enables a measurement of  $S(E)$  and  $T$  for the strongly interacting gas.

For our measurements of  $S(E)$ , the origin for  $S = 0$  is determined by the cloud sizes  $\hbar z_F^2 \dot{z}_0$

for the ground states at 840 G and 1200 G. These sizes are estimated from the data at the lowest temperatures. In the harmonic approximation, the ground state obeys  $\hbar z^2 i_0 = z_F^2 = (3/4)^{1/P} -$ , where  $1 +$  is the ratio of the energy per particle of the strongly interacting gas to that of a noninteracting gas with the same density (5, 6, 2, 1). At our lowest temperatures, including anharmonicity arising from the gaussian trapping potential  $U_{\text{trap}}$ , we find  $\epsilon_{\text{eff}} = 0.50(0.04)$  at 840 G. For our trap parameters, this corresponds to  $\epsilon = 0.54(0.04)$  at 834 G, using the estimate of Ref. (28). Our result is in good agreement with recent measurements based on the axial cloud size, where  $\epsilon = 0.54(0.02)$  (29),  $\epsilon = 0.54(+0.05/-0.12)$  (27) and with recent calculations,  $\epsilon = 0.56$  (7),  $\epsilon = 0.545$  (30),  $\epsilon = 0.564$  (28). Using our measured  $\epsilon_{\text{eff}} = 0.50$ , the ground state energy per particle for the strongly interacting gas is (20)  $E_0 = (3/4)^{1/P} E_F$ , yielding  $E_0 = 0.53 E_F$  and  $\hbar z^2 i_0 = z_F^2 = 0.55$  at 840 G.

We can predict the ground state cloud size at 1200 G using the equation of state at zero temperature. An approximate equation of state for the chemical potential versus local density,  $\mu(n)$ , is given in Ref. (28). Very good agreement with quantum Monte Carlo calculations is obtained for negative scattering lengths, which is the region of interest to us. We invert the equation of state to find  $n(\mu)$ , and then using  $\mu = \mu_g - U_{\text{trap}}$ , we determine the density for a gaussian potential  $U_{\text{trap}}$  to include anharmonicity. Normalization to the number of atoms yields the global chemical potential  $\mu_g$  and the mean square cloud size. At 1200 G, where  $k_F a_s = 0.75$ , we find  $\hbar z^2 i_0 = z_F^2 = 0.69$ . Our measurements at the lowest temperatures yield  $\hbar z^2 i_0 = z_F^2 = 0.72(0.02)$  at 1200 G, in agreement with the calculated value. Hence, at both 1200 G and 840 G, we obtain clouds nearly in the ground state and the corresponding cloud size ratio  $0.72/0.55 = 1.31$  shown in Fig. 1.

To convert the data of Fig. 1 into an entropy measurement, we calculate the entropy at 1200 G as a function of the ratio  $(\hbar z^2 i - \hbar z^2 i_0) = z_F^2$ , which is determined from the axial cloud size data at 1200 G. This method automatically assures that  $S = 0$  corresponds to the measured ground

state  $\hbar\omega_{\text{ho}}^2$  at 1200 G, and compensates for small shifts between the calculated and measured ground state sizes. Then,  $S[(\hbar\omega_{\text{ho}}^2 - \hbar\omega_{\text{ho}}^2) = \epsilon_F^2]$  is obtained from a many-body calculation at  $k_F a_s = 0.75$ , assuming an isotropic gaussian trapping potential, which automatically corrects for anharmonicity (25, 31). As discussed above, nearly identical results are obtained if we assume that the entropy at 1200 G is that of an ideal Fermi gas in the same potential.

Fig. 2 shows the entropy (blue dots) of the strongly interacting gas at 840 G as a function of its energy in the range  $0 \leq (E - E_0) = \epsilon_F$  to 1.4. The maximum energy is restricted to avoid evaporation in the shallow trap, which can reduce the energy and the atom number during the time of the magnetic field sweep. The entropy of the strongly interacting gas differs significantly from that of an ideal gas (lower orange dot-dash line), which has a larger ground state energy  $E_{\text{I0}} = 0.75 \epsilon_F$ , so that  $E_{\text{I0}} - E_0 = 0.22 \epsilon_F$ . To compare the curve shape for the measured entropy to that of an ideal gas, the ideal gas entropy is also plotted with its energy origin shifted, so that  $S = 0$  at  $E - E_0 = 0$  (upper orange dot-dashed line). In addition, the data are compared to predictions in the resonant regime based on pseudogap theory (25, 31) (dotted red line) and quantum Monte Carlo methods (dashed green line) (32, 33).

The temperature is determined in a model-independent manner from  $1/T = \partial S / \partial E$ . This requires parameterizing the  $S(E)$  data to obtain a smooth curve. The simplest assumption consistent with  $S(E - E_0) = 0$  is to approximate the data by a power law in  $E - E_0$ . However, one expects that below and above the superfluid transition at a critical energy  $E_c$ , the power law exponents will be different. This suggests the simple form,

$$\begin{aligned} S_{<}(E) &= k_B a \left( \frac{E - E_0}{\epsilon_F} \right)^b \quad \text{for } 0 \leq E - E_0 \leq E_c \\ S_{>}(E) &= S_{<}(E_c) + \left( \frac{E - E_0}{E_c - E_0} \right)^d \quad \text{for } E - E_0 \geq E_c; \end{aligned} \quad (2)$$

where the fit parameters are  $a, b, d$  and  $E_c$ . A fit with this parametrization yields a  $\chi^2$  per degree of freedom  $\chi^2 \approx 1$ , a factor of 2 smaller than that obtained by fitting a single power law to all of the

data. However, Eq. 2 ignores the smooth transition in slope near  $E_c$ , as required for continuity of the temperature, since the detailed critical behavior near  $E_c$  is not resolvable in our data.

Fitting the data of Fig. 2 with Eq. 2, the critical energy is found to be  $(E_c - E_0)/E_F = 0.41 \pm 0.05$ , with a corresponding critical entropy per particle  $S_c = 2.7( \pm 0.2) k_B$ . Below  $E_c$ , the entropy varies with energy as  $S_<(E) = k_B (4.6 \pm 0.2) [(E - E_0)/E_F]^{0.61 \pm 0.04}$ . Above  $E_c$ , we obtain  $S_>(E) = k_B (4.0 \pm 0.2) [(E - E_0)/E_F]^{0.45 \pm 0.01}$ . We find that the variances of  $a$  and  $b$  have a positive correlation, so that  $S(E)$  is determined more precisely than the independent variation of  $a$  and  $b$  would imply. The change in behavior near  $E_c$  is shown clearly in the inset of Fig. 2 and in the log-log plot of Fig. 3.

The power law exponent below  $E_c$ ,  $b = 0.61$ , falls between that of an ideal harmonically-trapped Fermi gas, where a Sommerfeld expansion at low energy yields  $S \propto (E - E_0)^{1/2}$  and that of an ideal harmonically-trapped Bose-Einstein condensate, where  $S \propto (E - E_0)^{3/4}$ . By contrast, above  $E_c$ , the exponent  $d = 0.45$ , is close to the result we obtain by fitting a power law to the entropy of an ideal gas, i.e.,  $S_I(E - E_{I0}) \propto (E - E_{I0})^b$ . In this case,  $b = 0.485$  for  $E - E_{I0}$  below  $0.41 E_F$  and  $b = 0.452$  above. This is consistent with the cloud size ratios shown in Fig. 1, which converge to unity at higher energies.

The fit parameters from the data can be compared to those obtained from fits to the theoretical curves shown in Fig. 2. The pseudogap theory (25, 31) predicts  $E_c - E_0 = 0.36 E_F$ , and  $S_c = 2.16 N k_B$ . Using Eq. 2 to fit the theoretical curve below the predicted  $E_c$ , we find  $S_<(E) = k_B (4.244 \pm 0.003) [(E - E_0)/E_F]^{0.61 \pm 0.005}$ . For the quantum Monte Carlo treatment (32, 33), which predicts  $E_c - E_0 = 0.32 E_F$ , we find  $S_c = 2.17 N k_B$ , and  $S_<(E) = k_B (4.35 \pm 0.05) [(E - E_0)/E_F]^{0.613 \pm 0.007}$ . Here the error estimates do not include the error in the theoretical curves. The small variances indicate that the power law fit closely approximates the theory, showing that Eq. 2 is a reasonable parametrization.

The energy versus temperature  $E(T)$  is determined from the derivative of the fit function



$S(E)$ . For  $E = E_c$ ,

$$\frac{E - E_0}{E_F} = \frac{abT}{T_F}^{\frac{1}{1-b}} : \quad (3)$$

From the best fit to the entropy data, where  $a = 4.6$ ,  $b = 0.61$ ,  $E_c = 0.41 E_F$ , we obtain  $(E - E_0)/E_F = 1.4 (T/T_F)^{2.56}$ .

We estimate the critical temperature  $T_c$  using the measured value of  $E_c - E_0 = (0.41 \pm 0.05) E_F$ . Here, we interpret  $E_c$  as the critical energy for the superfluid transition. We note that using  $E_0 = 0.53 E_F$  yields  $E_c = (0.94 \pm 0.05) E_F$ . This value is consistent with our previous measurements based on the heat capacity, where we observe a change in behavior at  $E = 0.85 E_F$  (20), and in collective mode damping (21), where a plot of the damping rate versus energy (rather than empirical temperature) shows a change in behavior near  $E = 1.01 E_F$ .

Ideally, to obtain  $T_c$ , the fit  $S(E)$  should have a continuous slope near  $E_c$ . Since our fit function has different slopes above and below  $E_c$ , we approximate the true slope by the average, as expected for the tangent to a smooth curve. Inverting Eq. 3 yields  $T/T_F = 0.36 [(E - E_0)/E_F]^{0.39}$  and  $T_{c<} = T_F = 0.25$ . Similarly, for  $E(T) > E_c$ , we find  $T/T_F = 0.56 [(E - E_0)/E_F]^{0.55}$  and  $T_{c>} = T_F = 0.34$ . Assuming that  $2 = T_c' = 1/T_{c<} + 1/T_{c>}$ , we find  $T_c = T_F = 0.29(0.02)$ . Here, the error estimate includes the cross correlations in the variances of  $a$ ,  $b$ ,  $E_c$ , and  $d$ .

The measured critical temperature  $T_c = T_F = 0.29(0.02)$  can be compared to our previous estimate of  $T_c = T_F = 0.27$  from an experiment with a model dependent temperature calibration (20). Moreover, the result 0.29 is in good agreement with predictions for trapped atoms, 0.29 (20), 0.30 (34), 0.31 (30), 0.30 (35), 0.26 (10) and 0.27 (32, 33).

Transition temperatures also have been predicted for a uniform gas,  $k_B T_c = E_F = 0.152$  (36) and  $k_B T_c = E_F = 0.160$  (37). These also can be compared to our measured  $T_c$ . Here  $E_F$  is the Fermi energy corresponding to the uniform density. By contrast, we determine the ratio  $T_c = T_F$ , where  $T_F$  is the Fermi temperature for a noninteracting gas at the center of a harmonic trap. If

we assume that  $\rho_F$  corresponds to the central density of the strongly interacting gas in our trap, then  $\rho_F = \rho - k_B T_F$  (20). From this, we estimate  $T_c = T_F = k_B T_c = (\rho_F)^{1/3}$ . For Ref. (36), we assume  $\rho = 0.44$  (7), and obtain  $T_c = T_F = 0.23$ . Ref. (37) calculates  $\rho = 0.36$  yielding  $T_c = T_F = 0.27$ .

## References and Notes

1. K. M. O'Hara, S. L. Hemmer, M. E. Gehm, S. R. Granade, J. E. Thomas, *Science* **298**, 2179 (2002).
2. H. Heiselberg, *Phys. Rev. A* **63**, 043606 (2001).
3. T.-L. Ho, *Phys. Rev. Lett.* **92**, 090402 (2004).
4. J. E. Thomas, A. Turlapov, J. Kinast, *Phys. Rev. Lett.* **95**, 120402 (2005).
5. G. F. Bertsch proposed the problem of determining the ground state of a two-component Fermi gas with a long scattering length and defined the parameter  $\eta$ .
6. G. A. Baker, Jr., *Phys. Rev. C* **60**, 054311 (1999).
7. J. Carlson, S.-Y. Chang, V. R. Pandharipande, K. E. Schmidt, *Phys. Rev. Lett.* **91**, 050401 (2003).
8. P. F. Kolb, U. Heinz, *Quark Gluon Plasma 3* (World Scientific, 2003), p. 634.
9. Q. Chen, J. Stajic, S. Tan, K. Levin, *Physics Reports* **412**, 1 (2005).
10. H. Hu, X.-J. Liu, P. D. Drummond, *Phys. Rev. A* **73**, 023617 (2006).
11. C. A. R. S. de Melo, M. Randeria, J. R. Engelbrecht, *Phys. Rev. Lett.* **71**, 3202 (1993).

12. M. Holland, S. J. J. M. F. Kokkelmans, M. L. Chiofalo, R. Walser, *Phys. Rev. Lett.* **87**, 120406 (2001).
13. E. Timmermans, K. Furuya, P. W. Milonni, A. K. Kerman, *Phys. Lett. A* **285**, 228 (2001).
14. C. A. Regal, M. Greiner, D. S. Jin, *Phys. Rev. Lett.* **92**, 040403 (2004).
15. M. W. Zwierlein, *et al.*, *Phys. Rev. Lett.* **92**, 120403 (2004).
16. J. Kinast, S. L. Hemmer, M. E. Gehm, A. Turlapov, J. E. Thomas, *Phys. Rev. Lett.* **92**, 150402 (2004).
17. T. Bourdel, *et al.*, *Phys. Rev. Lett.* **93**, 050401 (2004).
18. C. Chin, *et al.*, *Science* **305**, 1128 (2004).
19. G. B. Partridge, K. E. Strecker, R. I. Kamar, M. W. Jack, R. G. Hulet, *Phys. Rev. Lett.* **95**, 020404 (2005).
20. J. Kinast, *et al.*, *Science* **307**, 1296 (2005). Published online 27 January 2005 (10.1126/science.1109220).
21. J. Kinast, A. Turlapov, J. E. Thomas, *Phys. Rev. Lett.* **94**, 170404 (2005).
22. M. Zwierlein, J. Abo-Shaeer, A. Schirotzek, C. Schunck, W. Ketterle, *Nature* **435**, 1047 (2005).
23. M. Bartenstein, *et al.*, *Phys. Rev. Lett.* **94**, 103201 (2005).
24. To estimate the anharmonic correction to the energy, we use the approximation of an isotropic gaussian trapping potential  $U = U_0 [1 - \exp(-\frac{1}{2}r^2/(2U_0))]$ . In this case, we find  $\langle \frac{1}{2}m\omega^2 r^2 \rangle = (8U_0\hbar^2/a^2)$ . For total energies above  $E_F$ , where the spatial distribution is nearly gaussian, one readily obtains  $\langle \frac{1}{2}m\omega^2 r^2 \rangle = 3\hbar^2/a^2$  and  $\langle \frac{1}{2}m\omega^2 r^2 \rangle = (5E_F/8U_0)\hbar^2/a^2 = \frac{1}{2}m\omega_F^2 r_F^2$ .

25. Q. Chen, pseudogap theory of the entropy, energy and cloud size of a trapped Fermi gas, private communication.
26. C. A. Regal, C. Ticknor, J. L. Bohn, D. S. Jin, *Nature* **424**, 47 (2003).
27. J. T. Stewart, J. P. Gaebler, C. A. Regal, D. S. Jin, The potential energy of a  $^{40}\text{K}$  Fermi gas in the BCS-BEC crossover (2006). ArXiv:cond-mat/0607776.
28. C. Chin, *Phys. Rev. A* **72**, 041601(R) (2005).
29. G. B. Partridge, W. Li, R. I. Kamar, Y. Liao, R. G. Hulet, *Science* **311**, 503 (2006).
30. A. Perali, P. Pieri, G. C. Strinati, *Phys. Rev. Lett.* **93**, 100404 (2004).
31. Q. Chen, J. Stajic, K. Levin, *Phys. Rev. Lett.* **95**, 260405 (2005).
32. A. Bulgac, quantum Monte Carlo theory of the entropy and energy of a trapped unitary Fermi gas, private communication.
33. A. Bulgac, J. E. Drut, P. Magierski, *Phys. Rev. Lett.* **96**, 090404 (2006).
34. J. Kinnunen, M. Rodríguez, P. Törmä, *Science* **305**, 1131 (2004).
35. P. Massignan, G. M. Bruun, H. Smith, *Phys. Rev. A* **71**, 033607 (2005).
36. E. Burovski, N. Prokof'ev, B. Svistunov, M. Troyer, *Phys. Rev. Lett.* **96**, 160402 (2006).
37. R. Haussmann, W. Rantner, S. Cerrito, W. Zwerger, Thermodynamics of the BCS-BEC crossover (2006). ArXiv:cond-mat/0608282.
38. We thank Ingrid Kaldre for help in constructing the cold atom source. We are grateful to Qijin Chen and Kathy Levin, U. Chicago, and Aurel Bulgac and Joaquín E. Drut, U. Washington, Seattle, for providing calculations of the entropy versus cloud size in advance of

publication. We also thank Jason Ho for many discussions about entropy and energy measurement, which stimulated this work. This research is supported by the Chemical Sciences, Geosciences and Biosciences Division of the Office of Basic Energy Sciences, Office of Science, U. S. Department of Energy, the Physics Divisions of the Army Research Office and the National Science Foundation, and the Physics for Exploration program of the National Aeronautics and Space Administration.

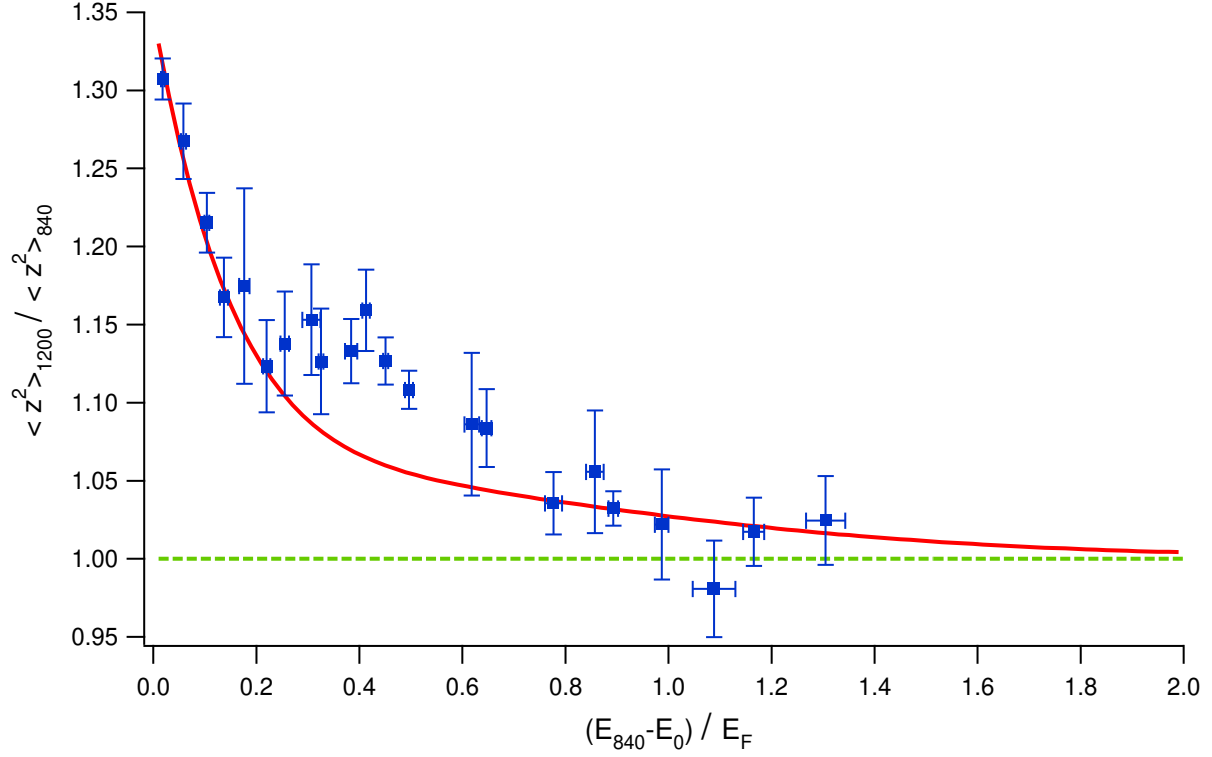


Figure 1: Ratio of the mean square cloud size at 1200 G,  $\langle z^2 \rangle_{1200}$  to that at 840 G,  $\langle z^2 \rangle_{840}$ . The data is obtained by adiabatically sweeping a bias magnetic field from 840 G, where the Fermi gas is strongly interacting, to 1200 G where it is weakly interacting.  $E_{840}$  is the total energy of the strongly interacting gas at 840 G prior to the sweep,  $E_0$  is the ground state energy at 840 G, and  $E_F$  the Fermi energy of a noninteracting gas. The solid line shows the theoretical prediction based on the calculated entropies (25). The ratio converges to unity at high energy, as expected (dashed green horizontal line).

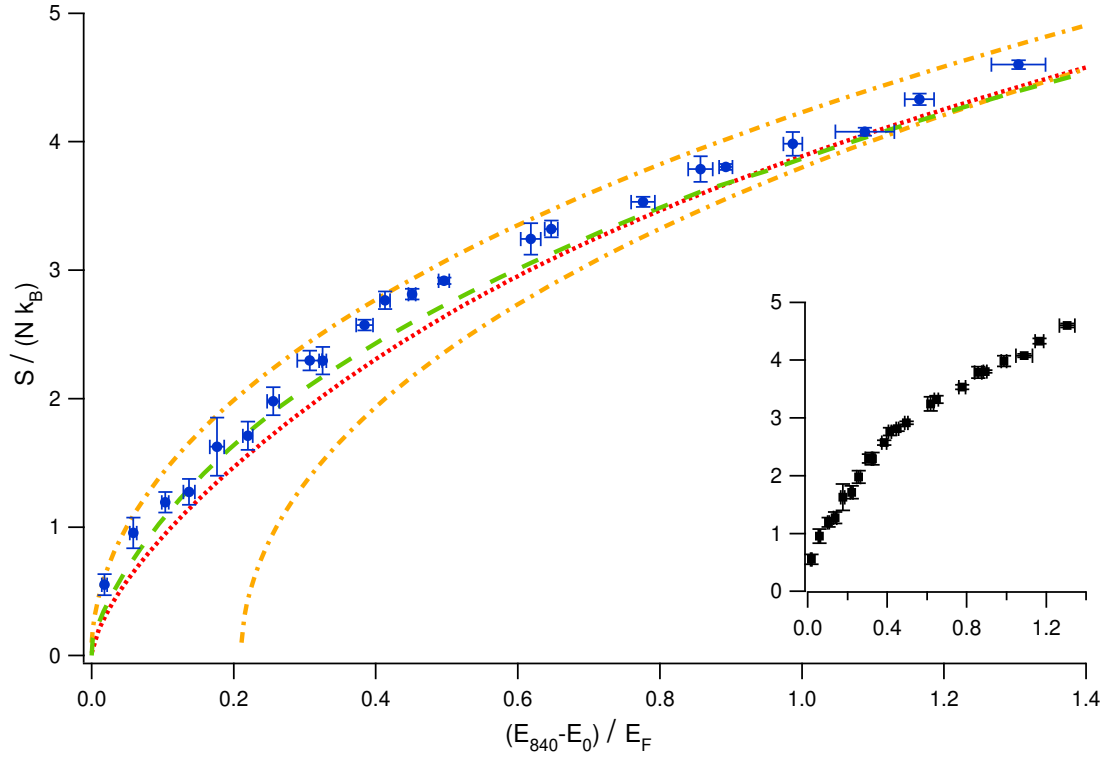


Figure 2: Measured entropy of a strongly interacting Fermi gas at 840 G versus its total energy (blue dots). The entropy is estimated from the measured cloud size at 1200 G after an adiabatic sweep of the magnetic field from 840 G. Lower orange dot-dashed curve– ideal gas entropy; Upper orange dot-dashed curve– ideal gas entropy with the ground state energy shifted to  $E_0$ ; Red dots– pseudogap theory (25); Green dashes– quantum Monte Carlo prediction (32). Inset– entropy versus energy data showing knee at  $E_c - E_0 = 0.41 E_F$ .

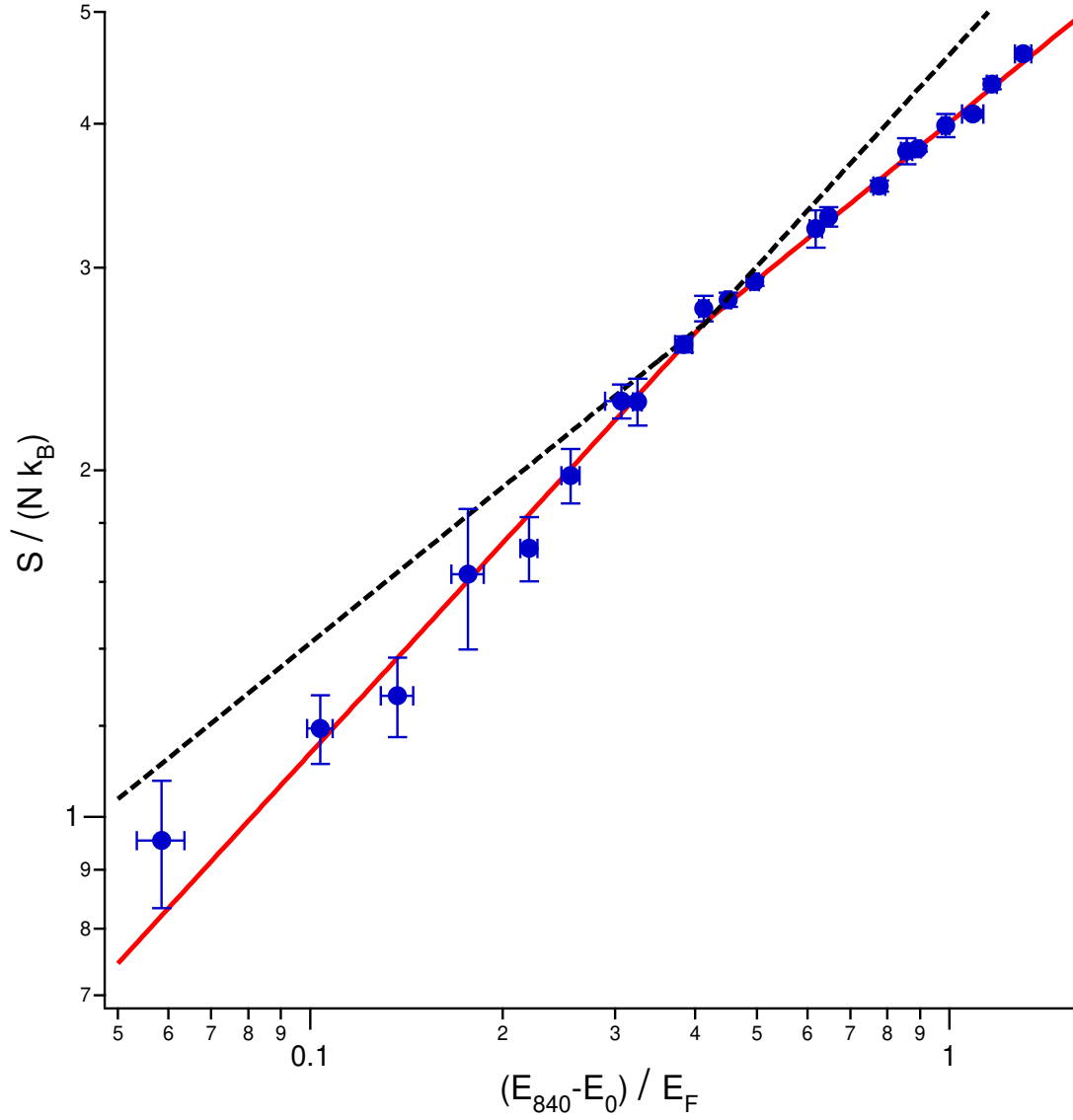


Figure 3: Power law fits for the measured entropy (blue dots) of the strongly interacting Fermi gas at 840 G versus its total energy, showing a transition in behavior. Red solid lines show the fitted power laws below and above  $E_c - E_0 = 0.41 E_F$ . Dotted black lines show the extended fits. Note that the fit function does not model the smooth transition in slope near the critical energy  $E_c$ , as required for continuity of the temperature.